Crossover between Ising and *XY*-like behavior in the off-equilibrium kinetics of the one-dimensional clock model

Natascia Andrenacci,* Federico Corberi,† and Eugenio Lippiello‡
Dipartimento di Fisica "E. Caianiello" and CNR-INFM Istituto Nazionale di Fisica della Materia, Università di Salerno, 84081 Baronissi (Salerno), Italy

(Received 17 May 2006; revised manuscript received 20 July 2006; published 13 September 2006)

We study the phase-ordering kinetics following a quench to a final temperature T_f of the one-dimensional p-state clock model. We show the existence of a critical value $p_c=4$, where the properties of the dynamics change. At $T_f=0$, for $p\leqslant p_c$ the dynamics is analogous to that of the kinetic Ising model, characterized by Brownian motion and annihilation of interfaces. Dynamical scaling is obeyed with the same dynamical exponents and scaling functions of the Ising model. For $p>p_c$, instead, the dynamics is dominated by a texture mechanism analogous to the one-dimensional *XY* model and dynamical scaling is violated. During the phase-ordering process at $T_f>0$, before equilibration occurs, a crossover between an early *XY*-like regime and a late Ising-like dynamics is observed for $p>p_c$.

DOI: 10.1103/PhysRevE.74.031111 PACS number(s): 05.70.Ln, 75.40.Gb, 05.40.−a

I. INTRODUCTION

After quenching a ferromagnetic system to a low-temperature phase, relaxation towards the new equilibrium state is realized by a progressive phase ordering [1]. The specific mechanisms involved in the coarsening phenomenon depend on the presence and on the nature of topological defects seeded by the disordered initial configuration which, in turn, are determined by the space dimensionality d and the number of components, N, of the order parameter. For $N<d$ defects are spatially extended; in this case coarsening is driven by reducing the typical curvature of the defect core, removal of sharp features, and shrinking of domain bubbles or vortex loops. Systems with $N=d$ are characterized by the presence of stable localized topological defects, and the ordering process occurs by mutual defect-antidefect annihilation. This is the case of the Ising chain quenched to a final temperature $T_f=0$, where up and down domains are separated by pointlike interfaces performing Brownian walks. When $N=d+1$, such as in the one-dimensional *XY* model, the kinetics is characterized by textures, spatially extended defects without a core, along which the order parameter rotates by 2π. Growth of the typical size of textures is a relevant mechanism at work in these systems. Finally, for $N>d+1$ topological defects are unstable and the dynamics is solely driven by the reduction of the excess energy related to the smooth rotations of the order parameter.

In any case, the development of order is associated with the growth of one or more characteristic lengths, with laws that, besides the specific mechanisms discussed above, depend on the conservation laws of the dynamics.

Generally, the late stage is characterized by dynamical scaling. This implies that a single characteristic length $L(t)$ can be associated with the development of order in such a way that configurations of the system are statistically independent of time when lengths are measured in units of $L(t)$. The characteristic length usually has a power-law growth $L(t)\propto t^{1/z}$. In systems with a nonconserved order parameter one generally finds $z=2$. In particular, this value is provided by the exact solution of the kinetic Ising chain [2] quenched to zero temperature.

However, there are cases where dynamical scaling is violated, notably the *XY* model in $d=1,2$. In $d=1$ this is related [3] to the presence of two lengths $L_w(t)$ and $L_c(t)$, associated with the texture length and with the texture-antitexture distance, growing with different exponents $z=4$ and $z=2$, respectively.

In this article, we investigate the interplay between two coarsening mechanisms—pointlike defect annihilation and texture growth—in the phase-ordering kinetics of the one-dimensional (1D) p-state clock model. This spin system reduces to the Ising model for $p=2$ and to the *XY* model for $p=\infty$. We study how the model with generic p interpolates between these limiting cases which, as discussed above, behave in a radically different way. In doing that, we uncover the existence of a critical value $p_c=4$, where the properties of the dynamics change abruptly. For $p\leqslant p_c$ the dynamics at $T_f=0$ is characterized by Brownian motion and annihilation of interfaces between domains, as in the Ising model. One has dynamical scaling with the same dynamical exponents and, interestingly, the same scaling functions of the Ising model. For $p>p_c$, instead, the dynamics is dominated by a texture mechanism analogous to the case with $p=\infty$, and dynamical scaling is violated.

In $d=1$ there is no possibility of ergodicity breaking except at $T=0$. At any finite temperature the equilibrium state is disordered with a vanishing magnetization and a coherence length $\xi(T)$ that diverges in the $T\to 0$ limit. If the system is quenched to a sufficiently low temperature, one has a coarsening phenomenon in a preasymptotic transient until the growing length associated with the development of order becomes comparable with $\xi(T_f)$. Since $\xi(T_f)$ diverges as $T_f\to 0$, the phase-ordering stage can be rather long. In this regime we show that activated processes restore, after a characteristic time $\tau_p^{cross}(T_f)$, the Ising behavior also in the cases with $p>p_c$.

*Electronic address: andrenacci@sa.infn.it
†Electronic address: corberi@na.infn.it
‡Electronic address: lippiello@sa.infn.it

This paper is organized as follows: In Sec. II we introduce the model and define the observable quantities that will be considered. In Sec. III we present the outcome of numerical simulations of the model with different p. In particular, quenches to $T_f=0$ or to $T_f>0$ will be discussed in Secs. III A and III B, respectively. Here we shed light on the crossover between the Ising and the XY universality class and provide an argument explaining its microscopic origin. A summary and the conclusions are contained in Sec. IV.

II. MODEL AND OBSERVABLES

The p-state clock model in one dimension is defined by the Hamiltonian

$$H[\sigma] = -J\sum_{i=1}^{\mathcal{N}} \vec{\sigma}_i \cdot \vec{\sigma}_{i+1} = -J\sum_{i=1}^{\mathcal{N}} \cos(\theta_i - \theta_{i+1}), \tag{1}$$

where $\vec{\sigma}_i$ is a two-component unit-vector spin pointing along one of the directions

$$\theta_i = \frac{2\pi}{p} n_i, \tag{2}$$

with $n_i \in \{1,2,\ldots,p\}$, $i=1,\ldots,\mathcal{N}$ are the sites of the lattice, and we assume periodic boundary conditions $\theta_{\mathcal{N}+1}=\theta_1$. This spin system is equivalent to the Ising model for $p=2$ and to the XY model for $p\to\infty$. In $d=1$ the system is ergodic except at $T=0$. At any finite temperature the equilibrium state is disordered with a vanishing magnetization and a coherence length $\xi(T)$ that diverges in the $T\to 0$ limit.

We consider a system initially prepared in a high-temperature uncorrelated state and then quenched, at time $t=0$, to a lower final temperature T_f. The dynamics is characterized by the ordering of the system over a characteristic length growing in time until, at time $\tau_p^{eq}(T_f)$, it becomes comparable to $\xi(T_f)$. At this point the final equilibrium state at T_f is entered. Quenching to $T_f=0$, since $\xi(0)=\infty$, one has $\tau_p^{eq}(T_f)=\infty$; therefore an infinite system never reaches equilibrium and the phase-ordering kinetics continues indefinitely. If the system is quenched to a sufficiently low temperature, since $\xi(T_f)$ is very large, the same behavior, as for $T_f=0$, can be observed over the time window $t<\tau_p^{eq}(T_f)$.

The power-law growth of the characteristic size of ordered regions depends on the specific mechanisms at work in the kinetic process. In the 1D Ising model with nonconserved order parameter—i.e., single-spin-flip dynamics—ordering is determined by the Brownian motion of the interfaces between up and down domains, which annihilate upon meeting. This leads to

$$L(t) \sim t^{1/z}, \tag{3}$$

with $z=2$. The same value is also expected [4] for $p\leqslant 4$.

The situation is different in the XY model in $d=1$. Here the order parameter is a vector which can gradually rotate with a low energy cost. A smooth 2π rotation of the phase θ is called a texture when the rotation is clockwise or antitexture when it is counterclockwise. The length over which this phase winding occurs will be denoted by $L_w(t)$. After a quench from a disordered state textures and antitextures are formed with equal probability. Then, there are points where the rotation of θ changes direction and the phase decoheres. We denote with $L_c(t)$ the characteristic length over which the phase remains coherent. It was shown [3] that $L_w(t)$ and $L_c(t)$ grow with a power law (3) but with different exponents. Specifically one has $z=4$ for $L_w(t)$ and $z=2$ for $L_c(t)$. The existence of these two lengths is at the heart of the scaling violations of the XY model.

Characteristic lengths can be estimated from the knowledge of the two-point equal-time correlation function

$$G(r,t) = \langle \vec{\sigma}_i(t) \cdot \vec{\sigma}_{i+r}(t) \rangle, \tag{4}$$

where $\langle\cdots\rangle$ means an ensemble average—namely, taken over different initial conditions and thermal histories. Due to space homogeneity, $G(r,t)$ does not depend on i. If there is a single characteristic length in the system, one has dynamical scaling [1], which implies

$$G(r,t) = g(x), \tag{5}$$

where $x=r/L(t)$. In the Ising model one finds [2]

$$g(x) = \mathrm{erfc}\{x\}, \tag{6}$$

with $L(t)=\sqrt{2t}$. For small x one has the Porod linear behavior $1-g(x)\sim x$, which is expected for systems with sharp interfaces [1]. From Eq. (5) one can extract a quantity $L_G(t)$ proportional to $L(t)$ from the condition

$$G(L_G(t),t) = \frac{1}{2}, \tag{7}$$

namely, as the half-height width of $G(r,t)$. In the XY model, $G(r,t)$ still obeys Eq. (5), with $x=r/L_w(t)$, $L_w(t)=2^{3/4}(\pi t)^{1/4}$, and [1]

$$g(x) = \exp\left\{-\frac{x^2}{\xi_i}\right\}. \tag{8}$$

Here ξ_i is the correlation length of the initial condition which, for a quench from a disordered state, is of the order of the lattice spacing. The Porod law is not obeyed, since instead of sharp interfaces one has smooth textures. Note that $G(r,t)$ has a scaling form, although dynamical scaling is violated. Scaling violations can be evidenced by considering different quantities such as, for instance, the autocorrelation function

$$C(t,s) = \langle \vec{\sigma}_i(t) \cdot \vec{\sigma}_i(s) \rangle. \tag{9}$$

In the Ising model this quantity can be cast in scaling form [2]

$$C(t,s) = h(y), \tag{10}$$

where $y=t/s$ and

$$h(y) = \frac{2}{\pi} \arcsin \sqrt{\frac{2}{1+y}}. \tag{11}$$

In the XY model, instead, one finds [3] the stretched exponential behavior

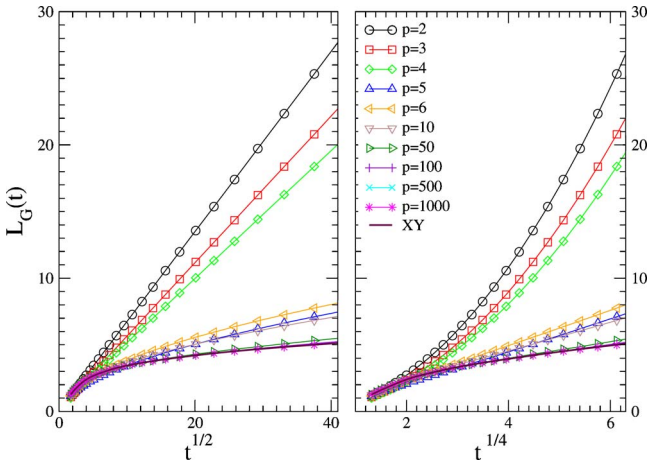

FIG. 1. (Color online) The characteristic length $L_G(t)$ is plotted against $t^{1/2}$ (left panel) and $t^{1/4}$ (right panel).

$$C(t,s) = \exp\left\{ -\frac{1}{\xi_i \sqrt{\pi}} s^{1/2} [2(y+1)^{1/2} - (2y)^{1/2} - \sqrt{2}] \right\}. \tag{12}$$

This expression cannot be cast in a scaling form, as for the Ising model, revealing the absence of dynamical scaling.

III. NUMERICAL RESULTS

In the following we will present the numerical results. Setting $J=1$, for each case considered we simulated a string of 10^4 spins with periodic boundary conditions and different values of p ranging from $p=2$, corresponding to the Ising model, to $p=\infty$, corresponding to the *XY* model. We consider a single-spin-flip dynamics regulated by transition rates

$$w\{[\sigma] \to [\sigma']\} = w_p\left(\frac{\Delta E}{T}\right) = \frac{2}{p \exp(\Delta E/2T) + \exp(-\Delta E/2T)}. \tag{13}$$

Here $[\sigma]$ and $[\sigma']$ are the spin configurations before and after the move, differing at most by the value of the spin on a randomly chosen site, $\Delta E = H[\sigma'] - H[\sigma]$, and we have set the Boltzmann constant to unity. The transition rates (13) are a generalization of Glauber transition rates to the p-state spins of the clock model. They reduce to the usual Glauber transition rates $w\{[\sigma]\to[\sigma']\} = (1/2)[1+\tanh(-\Delta E/2T)]$ for $p=2$. The factor $2/p$ in Eq. (13) ensures that all spin values have the same probability $1/p$ when $\Delta E = 0$.

An average over 10^4 realizations is made for each simulation. The statistical errors in the data reported in the figures are always smaller than the dimension of the symbols or the thickness of the lines.

A. Quenches to $T_f = 0$

Let us start with quenches to $T_f = 0$ by illustrating the behavior of the characteristic length $L_G(t)$ defined in Eq. (7). In Fig. 1 this quantity is plotted against $t^{1/2}$ (left panel) or against $t^{1/4}$ (right panel) for several values of p ranging from $p=2$ to $p=\infty$.

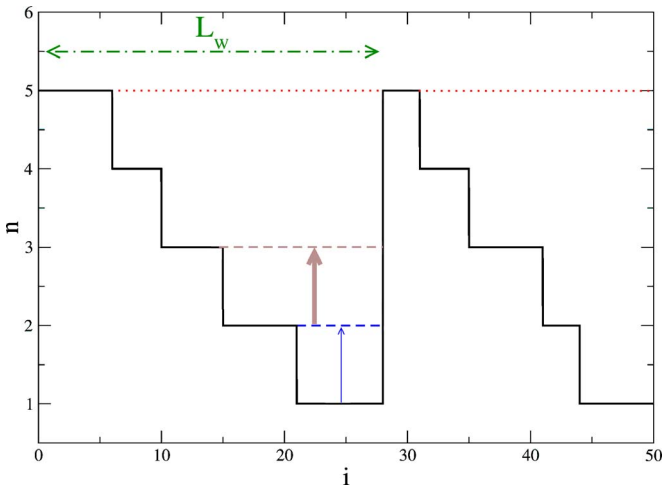

FIG. 2. (Color online) Schematic representation of a generalized texture for $p=5$.

This figure shows that $L_G(t)$ has an asymptotic power-law growth, as in Eq. (3), for every value of p. However, the dynamic exponent z radically changes going from $p \leqslant p_c$, where one has values very well consistent with $z=2$ (best fits yield $1/z = 0.49 \pm 0.01$ for $p=2,3,4$), to $p > p_c$ where $z=4$ is found with good accuracy (we find $1/z = 0.27 \pm 0.01, 0.27 \pm 0.01, 0.25 \pm 0.01$ for $p=5,6,10$). We recall that these are the values found in the Ising model and in the *XY* model. The behavior of $L_G(t)$, then, indicates a crossover from Ising to *XY* behavior upon crossing $p_c = 4$. We will see in the following that this is confirmed by the analysis of other dynamical quantities. Before doing that, however, let us discuss which is the microscopic mechanism at the basis of this crossover.

For finite values of $2 < p < \infty$ we generalize the definition of a texture as a region of the lattice of length $L_w(t)$ where p subsequent domains are found, each of average length $L_d(t) \sim L_w(t)/p$, such that moving along the lattice the value of n follows the sequence $n = p, p-1, \ldots, 1$. This is schematically shown in Fig. 2.

Two developed order-2 mechanisms are possible: A texture can grow by increasing the number of spins, $L_d(t)$, on every step. We anticipate that this process is found to be relevant for $p > p_c$ and leads to the power-law behavior (3) of $L_w(t)$ with $z=4$, as in the *XY* model. This behavior competes with the tendency to build the largest possible domains, instead of textures. This amounts to replace a texture with a number $N_D \ll p$ of domains each characterized by a single value of n. However, for $p > p_c$ at $T=0$, once textures are present, this process is not allowed. In fact, let us consider the situation of Fig. 2 and the possibility to form, in this region, a unique domain with, say, $n=p$ (the dotted line in Fig. 2). There are several ways to do this. Suppose one starts by rotating the spins with $n=1$ to $n=2$, as shown by the thin arrow in Fig. 2. After the move the energy would change by an amount

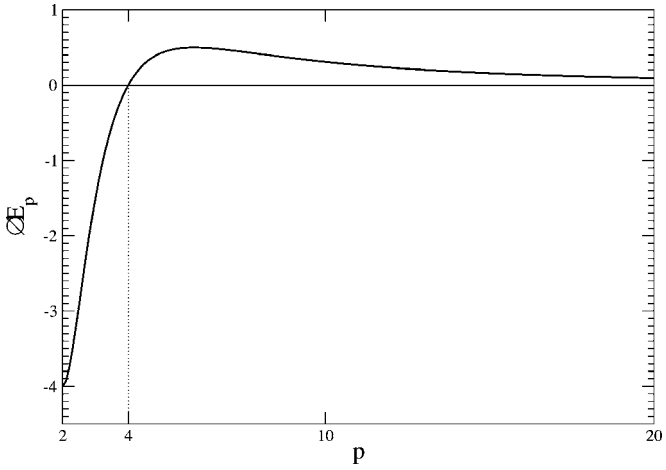

FIG. 3. The activation energy ΔE_p needed to destroy textures [Eq. (14)] is plotted against p.

$$\Delta E_p = J[2\cos(2\pi/p) - \cos(4\pi/p) - 1]. \quad (14)$$

This function is plotted in Fig. 3. Interestingly one has $\Delta E_p \leqslant 0$ or $\Delta E_p > 0$ for $p \leqslant p_c$ or $p > p_c$, respectively. At $T_f = 0$ moves with $\Delta E_p > 0$ are forbidden. Therefore, for $p > p_c$ there is no possibility to destroy the textures and form domains. Other possible moves, such as, for instance, a rotation from $n=1$ to $n=3$, correspond to a larger activation energy and are forbidden as well. Therefore, for $p > p_c$ textures and antitextures are stable against domain formation and the only ordering mechanism left is their growth and annihilation, much in the same way as in the XY model, leading to $z=4$. Conversely, for $p \leqslant p_c$ textures are removed and domains are created whose competition leads to the Ising-like behavior $z=2$. As already discussed, in the XY model the exponent $z=4$ is associated with the growth of the size of single textures. In order to check if the same mechanism is at work also in the clock model, in the numerical simulation we have identified the textures present in the system at each time and we have computed their average size $L_w(t)$. The results are shown in Fig. 4 for different values of

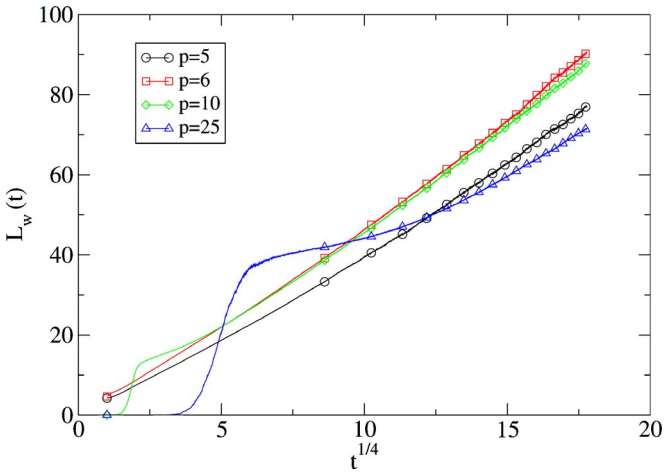

FIG. 4. (Color online) The average length of textures is plotted against $t^{1/4}$.

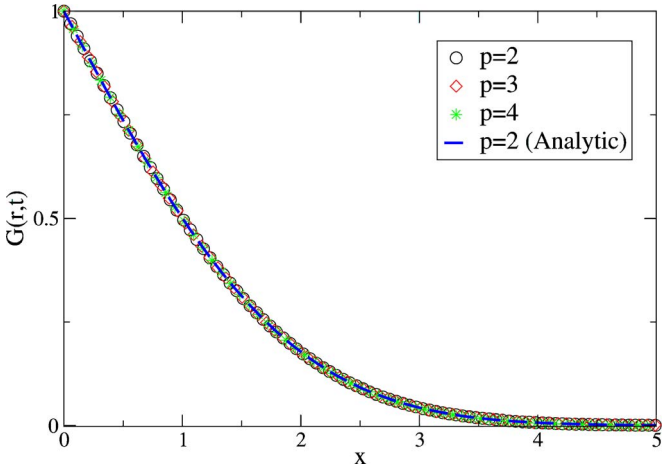

FIG. 5. (Color online) The correlation function $G(r,t)$ is plotted against $x=r/L_G(t)$ for $p=2,3,4$ at $t=1800$. The dashed line is the analytic expression (6).

$p > p_c$, showing that, actually, the size of textures grows as a power law $L_w \sim t^{1/z}$ with z quite compatible with $z=4$ (best fits yield $1/z=0.29\pm0.02, 0.29\pm0.02, 0.28\pm0.02, 0.23\pm0.02$ for $p=5,6,10,25$, respectively). This confirms that the exponent $z=4$ of the algebraic growth of $L_G(t)$ is determined by the texture mechanism, as in the XY model.

The previous results for $L_G(t)$ indicate the presence of a crossover at $p=p_c$ from the Ising to the XY nonequilibrium universality class. In order to substantiate this conjecture we have computed other dynamical quantities. The equal-time correlation function is plotted in Figs. 5–7 against $x = r/L_G(t)$. In Fig. 5 the cases with $p=2,3,4$ are considered. According to Eq. (5) for $p=2$ one should find a collapse of the curves with different s on a single master curve $g(x)$ given by Eq. (6). This is indeed observed in Fig. 5. According to our hypothesis the same behavior should be observed also for $p=3,4$, as can be verified in the figure. Moreover, one also finds that the master curves $g(x)$ are numerically

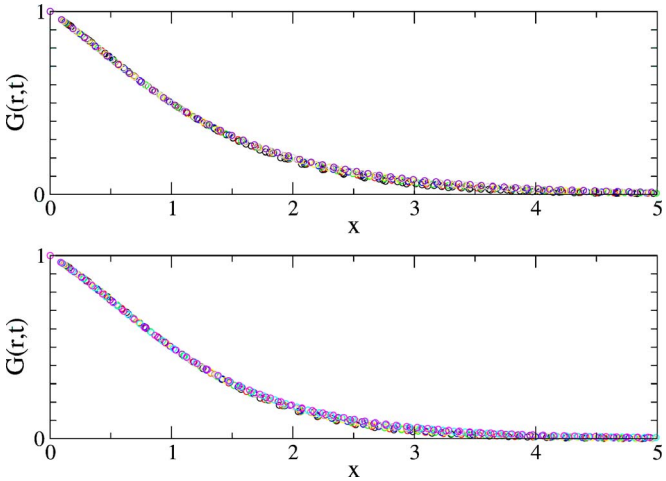

FIG. 6. (Color online) Data collapse of the correlation function $G(r,t)$ plotted against $x=r/L_G(t)$ for $p=5$ (upper panel) and $p=6$ (lower panel) at different times ($t=190, 245, 315, 405, 520, 665, 855, 1100, 1400, 1800$).

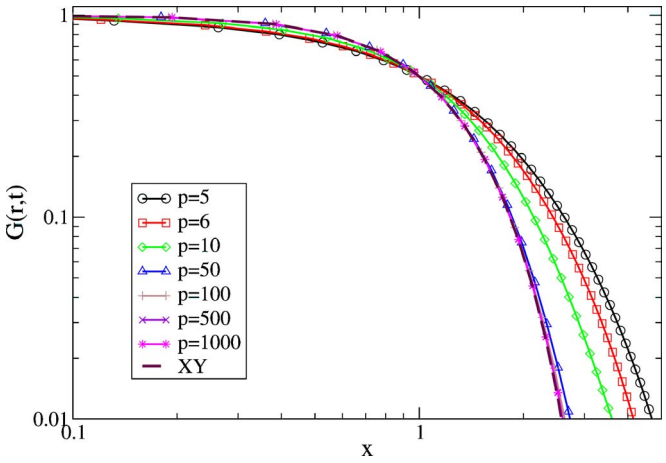

FIG. 7. (Color online) The correlation function $G(r,t)$ is plotted against $x=r/L_G(t)$ for different values of p at $t=1800$.

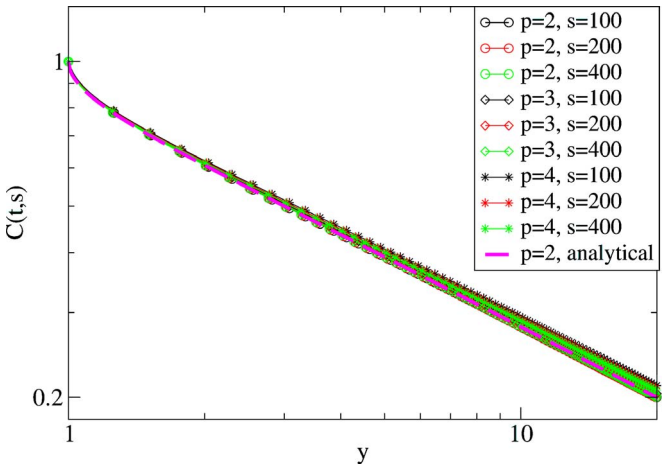

FIG. 8. (Color online) The autocorrelation function is plotted against y for $p=2,3,4$. The dashed line is the analytic expression (11).

indistinguishable for different p and they all coincide with that of Eq. (6). This result is trivial for $p=4$, since in this case the clock model can be mapped exactly on two noninteracting Ising models. The same property could be expected also for $p=3$. In fact, by considering $G(r,t)$, it easy (see the Appendix) to check that

$$G(r,t) = \frac{9}{2}G_P(r,t) - \frac{1}{2}, \tag{15}$$

where $G_P(r,t)$ is the *single-phase* equal-time correlation function of the three-state Potts model. This quantity was computed in Ref. [5], where it was found that

$$G_P(r,t) = \frac{2}{9}G_I(r,t) + \frac{1}{9}, \tag{16}$$

where $G_I(r,t)$ is the equal-time correlation function of the Ising model. Plugging Eq. (16) into Eq. (15) one finds $G(r,t)=G_I(r,t)$. The same argument also shows the identity between the two time correlation functions of the clock model with $p=3$ and the Ising model, strongly suggesting the complete equivalence between these models.

Let us emphasize that this result indicates a stronger similarity among the cases $p=2,3,4$ than a unique nonequilibrium universality class would imply, since not only the exponents are equal but the whole functional form of the scaling function. This results are in contrast with those of Ref. [6] where an approximate theory was used to show the dependence of $g(x)$ on p. However, the approximation used in Ref. [6] is expected to improve increasing the dimensionality d.

The cases with $p>p_c$ are shown in Figs. 6 and 7. As discussed in Sec. II, $G(r,t)$ obeys the scaling form (5) also in the *XY* model, although dynamical scaling is violated. According to our conjecture, for $p>p_c$ we expect the same behavior. In Fig. 6 it is shown that, indeed, the curves at different times collapse when plotted against $x=r/L_G(t)$. However, differently from the cases $p\leqslant p_c$, the masterfunction $g(x)$ depends on p and converges to the form (8) of the *XY* model for $p\to\infty$, as shown in Fig. 7.

Let us turn to consider the autocorrelation function, which is plotted in Figs. 8–10 against $y=t/s$. In Fig. 8 the cases with $p=2,3,4$ are considered. Here the situation is analogous to that of $G(r,t)$. For $p=2$ one should find a collapse of the curves with different s on a master curve $h(y)$, Eq. (10). This is indeed observed in Fig. 8. The same behavior is observed also for $p=3,4$. Again, as for $G(r,t)$, we find that the master curves $h(y)$ are numerically indistinguishable for different p and they all coincide with that of Eq. (11). In order to check if this property is completely general—namely, if every observable is characterized by the same exponents and scaling functions for $p=2,3,4$—besides the correlation functions we have also computed the integrated autoresponse function

$$\chi(t,s) = \int_s^t dt' R(t,t'). \tag{17}$$

Here

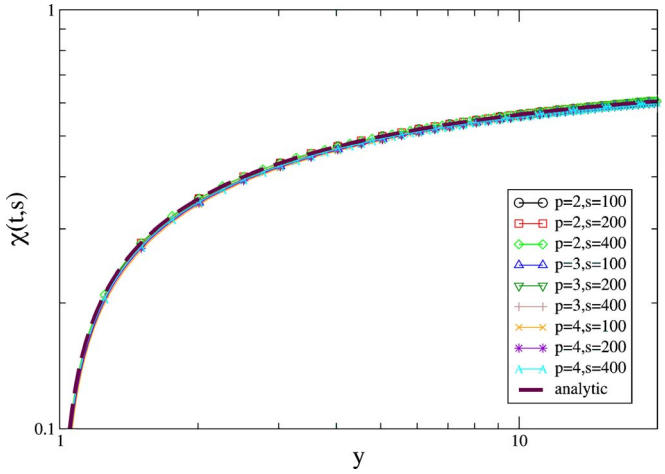

FIG. 9. (Color online) $\chi(t,s)$ is plotted against y for $p=2,3,4$. The dashed line is the analytic expression (20).

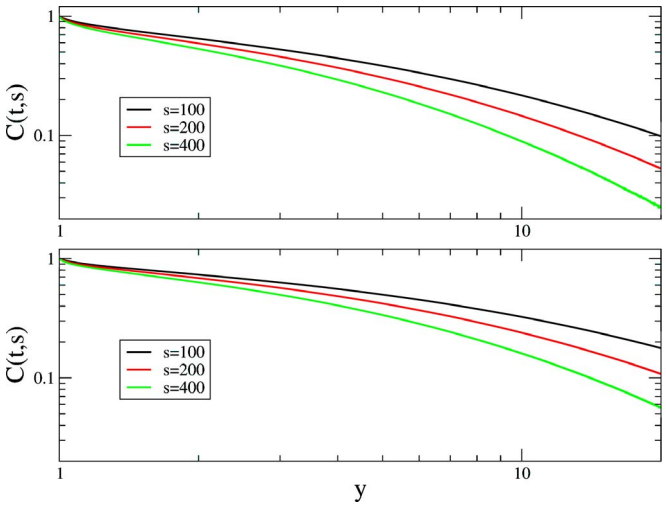

FIG. 10. (Color online) The autocorrelation function is plotted against y for $p=5$ (upper panel) and $p=6$ (lower panel).

$$R(t,t') = \sum_{\alpha} \left. \frac{\partial \langle \sigma_i^{\alpha}(t) \rangle}{\partial h_i^{\alpha}(t')} \right|_{\vec{h}_i=0}, \tag{18}$$

$\alpha=1,2$ being the generic vector components, is the linear autoresponse function associated with the perturbation caused by an impulsive magnetic field $\vec{h}_i$ switched on at time $t' < t$. In the Ising model [7], in the $T \to 0$ limit one finds

$$\chi(t,s) = f(t/s), \tag{19}$$

with

$$f(y) = \frac{1}{\sqrt{2}} \left(1 - \frac{2}{\pi} \arcsin \sqrt{y^{-1}} \right). \tag{20}$$

Here we measure the response function using the efficient method derived in Ref. [8] without applying the perturbation.

The behavior of $\chi(t,s)$ is shown in Fig. 9 for the cases $p=2,3,4$. One finds a collapse of the curves with different s on a master curve $f(y)$, as in Eq. (19) for $p=2$. Also in this case master curves $f(y)$ for different p are numerically indistinguishable. In conclusion, then, our data for $G(r,t)$, $C(t,s)$, and $\chi(t,s)$ confirm that the cases with $p=2,3,4$ share the same exponents and scaling functions. Notice that having the same scaling function both for $C(t,s)$ and $\chi(t,s)$, the cases with $p \leqslant p_c$ also have the same parametric plot of $\chi(t,s)$ versus $C(t,s)$ [7].

The situation is radically different for $p > p_c$. We expect here to see a texture-dominated XY-like dynamics, with violations of dynamical scaling that can be detected from $C(t,s)$. In fact, this is what one observes in Fig. 10, where the autocorrelation function is plotted against y. For each value of p, curves with different values of s do not collapse. The whole behavior is qualitatively similar to that of the XY model described by Eq. (12), which predicts a lowering of the curves for fixed y as s increases. Quantitatively, as already observed regarding $G(r,t)$, the analytic form of the curves depends on p and is different from that of the XY model—namely, Eq. (12). As shown in Fig. 11, Eq. (12) is gradually approached increasing p.

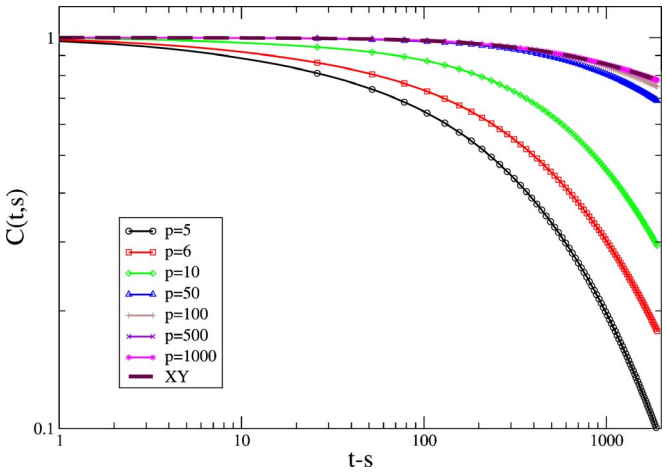

FIG. 11. (Color online) The autocorrelation function is plotted against y for $s=100$ and several values of p.

B. Quenches to $T_f > 0$

When quenches to finite temperatures are considered, as already discussed in Sec. II, one has a finite equilibration time $\tau_p^{eq}(T_f)$. In the following we will always discuss the ordering kinetics preceding the equilibration time—namely, for $t \ll \tau_p^{eq}(T_f)$.

According to our hypothesis, the XY-like behavior observed for $p > p_c$ is due to the impossibility to eliminate textures and form domains, because this would require activated processes with $\Delta E_p > 0$ given by Eq. (14). Quenching to a finite temperature those processes are no longer forbidden and we expect textures to start being removed after a characteristic time $\tau_p^{cross}(T_f)$. In order to estimate the crossover time let us consider again the situation of Fig. 3. The activated process described by the thin arrow, where the spins with $n=1$ are rotated to $n=2$, is a first action towards the removal of the texture, but the texture has not disappeared yet. The second action is the rotation of spins from $n=2$ to $n=3$, indicated by a bold arrow in the figure [9]. This requires an energy

$$\Delta E_p^{(2)} = J[\cos(2\pi/p) + \cos(4\pi/p) - \cos(6\pi/p) - 1]. \tag{21}$$

Then a third action is required, where spins with $n=3$ are rotated to $n=4$, and so on, until, after $p-1$ steps all the spins in the region considered have $n=p$. It is easy to generalize Eqs. (14) and (21) to the generic mth action:

$$\Delta E_p^{(m)} = J\{\cos(2\pi/p) + \cos(2m\pi/p) - \cos[2(m+1)\pi/p] - 1\}. \tag{22}$$

Let us consider $\Delta E_p^{(2)}$. This quantity is positive for $p > 6$. For

$p=5,6$, therefore, the second action is not an activated process, while it is activated for $p>6$. In general, from Eq. (22) one has $\Delta E_p^{(m)}>0$ for $p>2+2m$. The accomplishment of an action requires a time [10]

$$t_p^{(m)}(T_f) \simeq [w_p(\Delta E_p/T_f)]^{-1} = \frac{2}{p}\{1+\exp[\Delta E_p^{(m)}/T_f]\}, \tag{23}$$

w_p being the transition rates defined in Eq. (13). The crossover time—namely, the characteristic time after which textures are removed—is given by the sum of the times required for all the $p-1$ actions. It can be evaluated as

$$\tau_p^{cross}(T_f) = \sum_{m=1}^{p-1} t_p^{(m)}(T_f). \tag{24}$$

In the limit $T_f \to 0$ the sum is dominated by the process with the largest activation energy

$$\tau_p^{cross}(T_f \simeq 0) = \mathrm{Sup}_{\{m=1,p-1\}} t_p^{(m)}(T_f). \tag{25}$$

The Sup in this equation is obtained for $m=m^*$ given by

$$m^* = \begin{cases} 1 & \text{for } p<10, \\ \left[\dfrac{p-2}{4}\right] & \text{for } p \geqslant 10, \end{cases} \tag{26}$$

where $[x]$ is the integer part of x. Then, in the low-T limit one has

$$\tau_p^{cross}(T_f \simeq 0) = t_p^{m^*}(T_f). \tag{27}$$

In conclusion, for $p \leqslant p_c$ no activated processes are required and the system immediately enters the Ising-like phase ordering behavior. For $p>p_c$, instead, the dynamics is initially of the *XY* type until, at $t \sim \tau_p^{cross}(T_f)$, there is a crossover to the Ising-like nonequilibrium behavior.

The crossover can be appreciated in Figs. 12 and 13. The former shows the behavior of $L_G(t)$ for $p=6$ and different values of T_f. Here one observes initially the same behavior as for $T_f=0$—namely, $L_G(t) \propto t^{1/4}$—i.e., a straight line in the plot of $L_G(t)$ against $t^{1/4}$ (right panel). For larger times there is a crossover to Ising behavior $L_G(t) \simeq t^{1/2}$—namely, a straight line in the plot of $L_G(t)$ versus $t^{1/2}$ (left panel). Although the crossover is a quite smooth phenomenon, as can be seen in Fig. 12, $\tau_p^{cross}(T_f)$ given by Eq. (24), represented by thick segments across the lines, turns out to be of the correct order of magnitude for all the temperatures considered.

In Fig. 13 we plot $L_G(t)$ for $T_f=0.1$ and different values of p. One observes the same pattern of behavior of Fig. 12 with a crossover from a power-law growth with $z=4$ to one with $z=2$. The crossover time (24) grows with p, as expected.

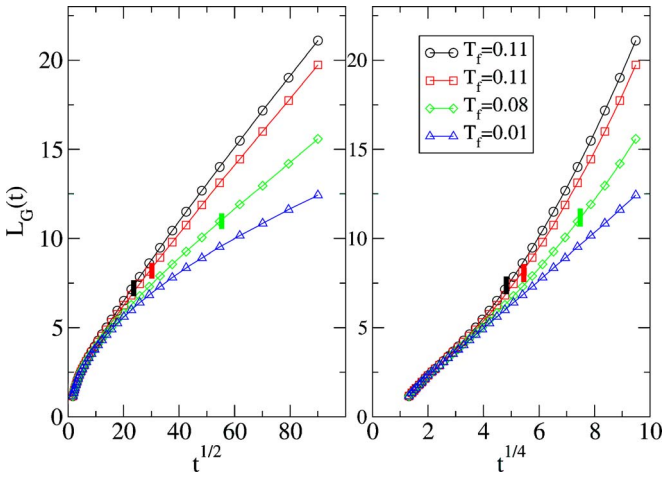

FIG. 12. (Color online) $L_G(t)$ is plotted against $t^{1/4}$ (left panel) or versus $t^{1/2}$ (right panel) for a quench of a system with $p=6$ and different values of T_f. Vertical segments on the curves for different T_f represent $\tau_p^{cross}(T_f)$ obtained from Eq. (24) as discussed in the text. For the smallest temperature $\tau_p^{cross}(T_f)$ is outside the range of times of the figure.

IV. CONCLUSIONS

In this paper we have studied the phase-ordering kinetics of the one-dimensional p-state clock model. We have shown the existence of a critical value $p_c=4$ separating two radically different dynamical behaviors. For $p \leqslant p_c$ the dynamics is in all respects analogous to that of the Ising model with $p=2$. Phase ordering proceeds by means of the formation and subsequent growth of domains through interface diffusion and annihilation. This similarity goes beyond the qualitative level: we find the same exponent and scaling functions for every $p \leqslant p_c$ and for all the one-time or two-time quantities considered. This reflects a deeper similarity than what a unique universality class, involving only the value of the exponents, would imply. For $p>p_c$ the dynamics changes dramatically, due to the relevant role played by textures. While for $p \leqslant p_c$ textures are quickly removed by means of nonactivated processes, for $p>p_c$ their removal can only be realized through activated processes. For quenches to $T_f=0$,

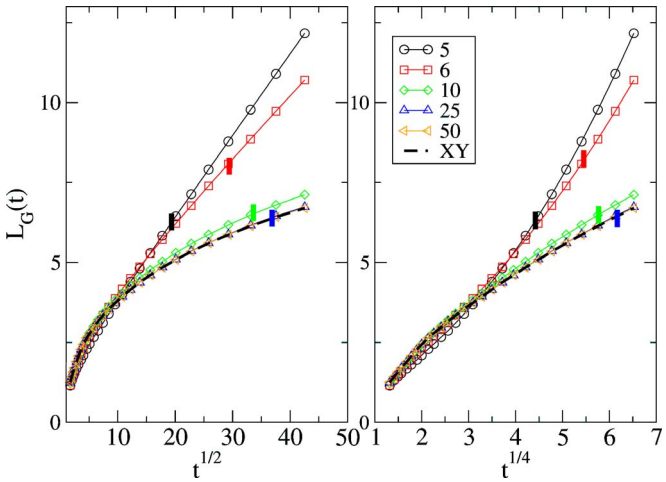

FIG. 13. (Color online) $L_G(t)$ is plotted against $t^{1/4}$ (left panel) or versus $t^{1/2}$ (right panel) for a quench at $T_f=0.1$ and several values of $p>p_c$. Vertical segments on the curves for different p represent $\tau_p^{cross}(T_f)$. For $p>25$ $\tau_p^{cross}(T_f)$ is outside the range of times of the figure.

activated processes are forbidden, and, therefore, textures remain in the system up to the longest times. Their peculiar growth mechanisms characterize the dynamics, similarly to what happens in the one-dimensional XY model, with the notable feature of violation of dynamical scaling and the anomalous growth with $z=4$ of the winding length $L_w(t)$. For quenches to finite T_f, textures survive up to a characteristic time $\tau_p^{cross}(T_f)$ which can be rather long for small temperatures or large p. A crossover phenomenon is then observed from an initial dynamics of the XY type to a later Ising-like behavior.

Our results are at odds with what is found in Ref. [6] where an approximate analytical solution of the clock model in arbitrary dimension is obtained, finding an analogous scaling behavior for all $p<\infty$ but with p-dependent scaling functions. In the present one-dimensional case, instead, the situation is the opposite. There is not an analogous scaling behavior for all values of p, but a qualitative difference occurs crossing p_c. In addition, when scaling holds—namely, for $p \leqslant p_c$—the scaling functions do not depend on p. We believe, however, the behavior of the system considered in this paper to be peculiar. Actually, the different dynamics observed crossing p_c is determined by the simultaneous presence of interfaces and textures. On the basis of the discussion of Sec. I we expect a similar situation to be only realized in N-component vectorial models with discrete states and $N=d+1$, where extended defects without a core may exist. For instance, it would be very interesting to study if a similar pattern is observed in $d=2$ for a generalization of the clock model where a three-component order parameter is only allowed to point on a finite number p of directions. In addition, we expect the remarkable feature of unique scaling functions for different values of p to be peculiar to the one-dimensional case. Considering the function $G(r,t)$, for instance, the scaling function describes the spatial distribution of domains and it is quite evident that in $d>1$ this depends on p. Taking the case $d=2$, for simplicity, one has the usual bicontinuous domain structure of domains and interfaces for $p=2$, while for $p>2$ there is a different pattern with interfaces and vortices [11]. However, in the one-dimensional case interfaces are pointlike objects for all values of p and one does not expect relevant differences in their spatial distribution when p is changed.

Finally, it would be very interesting to study if a similar pattern is observed in the one-dimensional clock model with a conserved order parameter. Concerning the value of the growth exponent z, which in the nonconserved case considered here effectively discriminate the Ising dynamics with $z=2$ from the XY behavior with $z=4$, in the conserved case one should observe a crossover from $z=3$ to $z=6$ [1,3].

ACKNOWLEDGMENTS

We acknowledge Dr. Clement Sire for valuable suggestions. This work has been partially supported from INFM through PAIS and from MURST through PRIN-2004.

APPENDIX

For the three-state clock model the correlation between two spins at a certain time t can be written as

$$G(r,t)=\langle \sigma_i \sigma_j \rangle = \sum_{n,n'=1,3} \cos[\theta_i(n)-\theta_j(n')] \times P_i(n,t) P_{i,j}(n,t|n',t), \tag{A1}$$

where r is the distance between i and j. Here n and θ_i (and their relation) are defined in Eq. (2), $P_i(n,t)$ is the probability to find the spin on site i in the state n at time t, and $P_{i,j}(n,t|n',t)$ is the conditional probability to find the state n' on site j provided that the state n is found in i. Isolating the diagonal terms one has

$$G(r,t)=\sum_{n=1,3} P_i(n,t) P_{i,j}(n,t|n,t) - \frac{1}{2} \sum_{n=1,3} P_i(n,t) \sum_{n' \neq n} P_{i,j}(n,t|n',t), \tag{A2}$$

where we have used the value $\cos(\theta_i-\theta_j)=-1/2$ when $\theta_i \neq \theta_j$. Since $\Sigma_{n' \neq n} P_{i,j}(n,t|n',t)=1-P_{i,j}(n,t|n,t)$, one has

$$G(r,t)=-\frac{1}{2} \sum_{n=1,3} P_i(n,t) + \frac{3}{2} \sum_{n=1,3} P_i(n,t) P_{i,j}(n,t|n,t) = -\frac{1}{2} + \frac{3}{2} \sum_{n=1,3} P_i(n,t) P_{i,j}(n,t|n,t). \tag{A3}$$

Let us turn now to the Potts model where a generic spin on site i can be found in the states labeled with $m_i=1,2,3$. Following Ref. [5], we define an auxiliary field $\phi_i(n)$ such that $\phi_i(n)=1$ if $m_i=n$, where n is a reference state, and $\phi_i(n)=0$ otherwise. The correlation of the auxiliary field is the *single-phase* correlation function of the Potts model and can be written as

$$G_n(r,t)=\langle \phi_i(n) \phi_j(n) \rangle = P_i(n,t) P_{i,j}(n,t|n,t), \tag{A4}$$

where the probabilities are defined analogously to those of the clock model introduced above. Recognizing $G_n(r,t)$ in the last term of the right-hand side of Eq. (A3) one arrives at

$$G(r,t)=-\frac{1}{2}+\frac{3}{2} \sum_{n=1,3} G_n(r,t). \tag{A5}$$

Because of the rotational symmetry, one has $G_P(r,t)=G_n(r,t)$ for all values of n and then one recovers Eq. (15).

[1] A. J. Bray, Adv. Phys. **43**, 357 (1994).
[2] R. J. Glauber, J. Math. Phys. **4**, 294 (1963).
[3] A. D. Rutenberg and A. J. Bray, Phys. Rev. Lett. **74**, 3836 (1995).
[4] F. Leyvraz and N. Jan, J. Phys. A **19**, 603 (1986).
[5] C. Sire and S. N. Majumdar, Phys. Rev. Lett. **74**, 4321 (1995); Phys. Rev. E **52**, 244 (1995).
[6] F. Liu and G. F. Mazenko, Phys. Rev. B **47**, 2866 (1993).
[7] E. Lippiello and M. Zannetti, Phys. Rev. E **61**, 3369 (2000).
[8] E. Lippiello, F. Corberi, and M. Zannetti, Phys. Rev. E **71**, 036104 (2005). Here the algorithm for the computation of the response function was obtained making explicit reference for simplicity to the case $p=2$, but the same derivation applies as well to generic p.
[9] As for the first action, other possible moves require a larger activation energy and are, therefore, suppressed at low temperatures.
[10] In a texture there may be several adjacent spins with the same value of n on a step, as in Fig. 2. Since the accomplishment of an action requires all these spins to be rotated, a number of elementary moves with $\Delta E=0$ may occur besides the (possibly) activated processes with energy variation $\Delta E_p^{(m)}$. These moves correspond to the Brownian displacement of the boundaries between, say, spins with $n=2$ and $n=3$ in Fig. 2. They can be disregarded in the computation of $t_p^m(T_f)$ at low temperatures since they require a microscopic time to occur.
[11] K. Kaski and J. D. Gunton, Phys. Rev. B **28**, 5371 (1983); K. Kaski, M. Grant, and J. D. Gunton, *ibid.* **31**, 3040 (1985).